A facile dip-coating process for preparing highly durable superhydrophobic surface with multi-scale structures on paint films

Cui, Zhe; Yin, Long; Wang, Qingjun; Ding, Jianfu; Chen, Qingmin

Publisher's version / Version de l'éditeur:
https://doi.org/10.1016/j.cis,2009.05.061
Journal of Colloid and Interface Science, 337, 2, pp. 531-537, 2009-09-15

Journal of Colloid and Interface Science 337 (2009) 531–537

Contents lists available at ScienceDirect

Journal of Colloid and Interface Science

www.elsevier.com/locate/jcis

A facile dip-coating process for preparing highly durable superhydrophobic surface with multi-scale structures on paint films

Zhe Cui [a], Long Yin [a], Qingjun Wang [a], Jianfu Ding [b,*], Qingmin Chen [a,*]

[a] Polymer Science and Engineering Department, School of Chemistry and Chemical Engineering, State Key Laboratory of Coordination Chemistry, Nanjing University, 22 Hankou Road, Nanjing, Jiangsu 210093, China

[b] Institute for Chemical Process and Environmental Technology, National Research Council Canada, 1200 Montreal Road, Building M-12, Ottawa, Ont., Canada K1A 0R6

ARTICLE INFO

Article history:
Received 8 October 2008
Accepted 20 May 2009
Available online 2 June 2009

Keywords:
Superhydrophobic
Multi-scale structure
Epoxy paint
pH and solvent resistance
High speed scouring resistance

ABSTRACT

Superhydrophobic surfaces with multi-scale nano/microstructures have been prepared on epoxy paint surfaces using a feasible dip-coating process. The microstructures with 5–10 μm protuberances were first prepared on epoxy paint surface by sandblast. Then the nanostructures were introduced on the microstructure surface by anchoring 50–100 nm SiO_2 particles (nano-SiO_2) onto the sandblasted paint surface, which was completed by dip-coating with a nano-SiO_2/epoxy adhesive solution (M1). At last the surface was further modified for enhancing hydrophobicity by another dip-coating with a solution of a low surface energy polymer, aminopropyl terminated polydimethylsiloxane (ATPS) modified epoxy adhesive (M2). The water contact angle of the as-prepared samples reached as high as 167.8° and the sliding angle was 7°. The prepared superhydrophobic surface exhibited excellent durability to the high speed scouring test and high stability in neutral and basic aqueous solutions and some common organic solvents. In addition, this method can be adopted to fabricate large scale samples with a good homogeneity of the whole surface at very low cost.

1. Introduction

A superhydrophobic surface is usually at a combination of two extreme regimes, Cassie and Wenzel regimes [1,2]. At Cassie regime, a water droplet is "suspended" on the surface as a sphere, where water does not intrude into the valley of the microstructures, so that air is trapped between the water droplet and the substrate. Therefore, this type of the surface acts as a "composite surface" of solid and air. The apparent contact angle of this surface, θ' can be estimated from the contact angle of the smooth surface, θ by the Cassie equation,

$$\cos\theta' = f_1(\cos\theta + 1) - 1 \tag{1}$$

where f_1 represents the fractions of solid–liquid contact area.

At the Wenzel regime, a water droplet can wet the whole microstructure surface, so that no air is trapped between water and the solid. In this case, the apparent contact angle of the rough surface, θ' correlates with the surface roughness and contact angle of the smooth surface, θ, following the Wenzel equation:

$$\cos\theta' = r\cos\theta \tag{2}$$

where r, defined as the roughness factor, is a ratio of the actual to apparent solid–liquid contact area. Apparently at this regime, the apparent contact angle of the rough surface will be normally increased with the increase of the roughness. Therefore increasing the surface roughness for the hydrophobic surface with θ larger than 90° should be an efficient way to achieve a high contact angle at the Wenzel regime. Consequently, no matter in which regime of a superhydrophobic surface, its apparent contact angle always depends on the intrinsic hydrophobicity of the material represented by its contact angle, θ and its rough surface structure.

Although a surface at either of these regimes can produce a high apparent contact angle, the sliding angle of a water droplet on either of these surfaces is significantly different. The sliding angle is depended on the interaction strength between water and solid, which can be described by Furmidge equation in the term of receding (θ_r) and advancing (θ_a) contact angles of the water droplet [3],

$$mg\mathrm{Sin}\,\alpha = \sigma w(\cos\theta_r - \cos\theta_a) \tag{3}$$

where α is the sliding angle, σ is the surface tension of water, and m and w are the weight and the width of the contact circle of the water droplet, and g is the gravitational acceleration. In this equation, the left side represents the gravity force, and the right side represents the capillary force. There the term in the bracket is actually a measure of the interaction strength between water and solid on the interface. Apparently on the Cassie surface, the actual water/solid contact area is very small and the value of this term is very low,

* Corresponding authors. Fax: +1 613 991 2384 (J. Ding); +86 25 83593048 (Q. Chen).
E-mail addresses: jianfu.ding@nrc-cnrc.gc.ca (J. Ding), chenqm@nju.edu.cn (Q. Chen).

0021-9797/$ - see front matter Crown Copyright © 2009 Published by Elsevier Inc. All rights reserved.
doi:10.1016/j.jcis.2009.05.061

which will result in a small sliding angle. While on the Wenzel surface, the actually contact area is much larger than the apparent area; a much higher interaction strength will be created at the interface. At this regime, a surface with a very high contact angle is possible to have a large sliding angle.

A surface with a water contact angle larger than 150° and a water sliding angle smaller than 10° is commonly considered as superhydrophobic surface to have self-cleaning property [4]. The phenomenon of superhydrophobicity universally exists in nature, such as the leaf surfaces of many plants [5,6] and the legs of water striders [7]. These surfaces have attracted many attentions in recent years due to their special properties such as anti-contamination, self-cleaning and nonstick, which are desirable for many applications including antibiofouling paints for boats [8], snow and ice rain nonstick coating for antennas, airplane and power line [9], self-cleaning coating for automobiles and architectures [10]. This property is related to the special multi-scale nano/microsurface structures and this correlation is widely known as the lotus effect [6,11–13]. In recent years, many technologies including electrochemical deposition [14–16], chemical [17–22] and plasma etching [23–25], electrospinning [26–28], and lithograph [29,30] are utilized to fabricate superhydrophobic surface by mimicking the lotus surface structure.

Although great successes have been made in the preparation of such structures, and superhydrophobic surfaces with an apparent contact angle close to 180° have been prepared from many different techniques [13,31], the successful applications of these man-made superhydrophobic surface are still at the premature stage, mainly due to the lack of facile ways for large scale fabrication and insufficient durability of the prepared superhydrophobic structures [32–37]. For example, many superhydrophobic surface are directly built up on metal surfaces [16–21], which are not stable in the conditions for many of above mentioned applications because these condition are usually corrosive to metal and can easily destroy the superhydrophobic structures. Therefore, for many of these applications, to create superhydrophobic surfaces on paint surfaces will be more promising than on the metal surface.

In this paper, we propose a facile process to prepare superhydrophobic structures on paint surfaces. Fig. 1 illustrated the idea to create the multi-scale nano/microstructures. The sample was prepared in three-steps (sandblasting/anchoring nano-SiO_2/dip-coating low surface energy polymer solution), where the microstructures were first built up on a paint surface by sandblasting, then nanostructures were anchored onto the surface of the microstructures by dip-coating a nano-SiO_2/polymer solution. The prepared surfaces were further modified by dip-coating with a low surface energy polymer solution. This process is easily applicable for large scale sample fabrication. The influence of the preparation conditions on the superhydrophobicity of the produced surfaces, and their resistances to external forces, to acidic and caustic aqueous solutions and organic solvents have been discussed. The produced surface displayed promising superhydrophobic properties with an apparent contact angle of 167° and a sliding angle of 7° and a high durability in a high speed water scouring test.

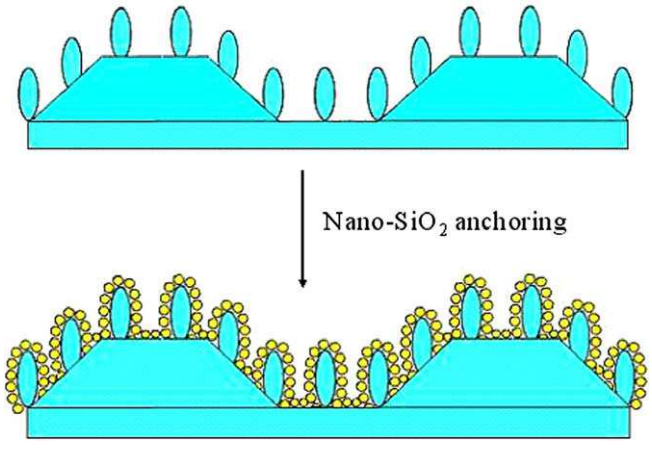

Fig. 1. Schematic illustration of the multi-scale structures prepared on the sandblasted paint surface by nano-SiO_2 anchoring.

2. Experimental section

2.1. Materials

The following starting materials were used as received: a bisphenol-A epoxy resin (E-44, epoxy equivalent: 210–240 g/eq, Wuxi Resin Factory, China); fumed SiO_2 nano-particles (nano-SiO_2, diameter, 10–15 nm, CAB-O-SIL EH-5, Cabot Co.); aminopropyl terminated polydimethylsiloxane (ATPS, Mn = 3000 Da, NH_2 content = 0.67 mmol/g, Henkel Int.); dimethylthiotoluenediamine, (E-300, Albemarle Co. USA) and 2,4,6-tri-(dimethylaminemethyl)phenol, (DMP-30, Sigma–Aldrich). The common chemicals including acetone, ethyl acetate (Sinopharm Chemical Reagent Co., Ltd China), ethanol, toluene, hydrochloric acid (Nanjing Chemical Regent Co., Ltd China), sodium hydroxide (Shanghai Lingfeng Chemical Regent Co. China) are analytical regents and used without further purification. Epoxy paint was kindly supplied by Polymer Engineering Material Research Center of Nanjing University.

2.2. Sample preparation

Stainless plates in sizes of 10 × 10, 20 × 20, 120 × 40 mm^2 were coated with epoxy paint by spray coating, and cured at room temperature for one day. The thickness of the paint films is between 100 and 200 μm. For creating superhydrophobic surface, the first step is to create microstructures on the paint surface. So that the paint surface was sandblasted using brown aluminum oxide grains (60 mesh) at the air pressure of 0.8 MPa, and washed with distilled water ultrasonically till completely removal of the grains, and then dried at room temperature.

The second step is to anchor nano-SiO_2 onto the prepared microstructure surface by dip-coating with the nano-SiO_2/epoxy adhesive (M1) solution, where the sandblasted sample was dip-coated in M1 solution twice, then cured at 60 °C for 2 h to form M1 coated surface. M1 solution was prepared by mixing the following two solutions (a nano-SiO_2 solution and an epoxy solution) in 1:1 ratio. The nano-SiO_2 solution was prepared by suspending desired amount (typically 1.0 g) of nano-SiO_2 in 100 mL of acetone, which was ultrasonicated until it became gelatinous. The epoxy solution was prepared by mixing E-44 (1.0 g, 0.0044 eq), E-300 (0.2 g, 0.0037 eq) and DMP-30 (five drops) in 100 mL of acetone.

Then the nano-SiO_2 anchored surface was further modified in the third step by dip-coating with an ATPS modified epoxy adhesive (M2) solution, and cured at 100 °C for 6 h for forming M2 coated surface. A series of M2 solutions with different concentration was prepared by mixing E-44 (0.3 g, 0.00132 eq), ATPS (0.15 g, 0.00020 eq), E-300 (0.05 g, 0.00094 eq) and DMP-30 (two drops) in 50 mL of acetone followed by diluting until the desired ATPS concentration was reached.

2.3. Characterization and instruments

Water contact angles and sliding angles were measured by a contact angle meter (Cam 200, KSV Instrument Ltd.) at 24 °C. A droplet of water in a size of 5 μL or 10 μL was used to test static

contact angle or sliding angle, respectively. The titling speed of the sample stage for the sliding angle measurement was 0.1°/s. The morphology of the samples was observed by means of field-emission scanning electron microscopy (SEM, LEO1530VP, Germany). High speed scouring test is conducted in a water bath equipped with a 16-face rotor (diameter: 52 mm). The as-prepared (10 mm × 10 mm) sample was fixed onto one face of the rotor, which was then rotated in distilled water at a speed of 10 m/s (3700 rpm). After scouring, the sample was dried in an oven at 100 °C, and then the contact angle was measured again at room temperature.

3. Results and discussion

3.1. The microstructures prepared by sandblasting

In order to prepare multi-scale superhydrophobic surfaces, microstructures are first created on the epoxy paint surface by sandblasting. The static contact angle of the paint surface increased from 77.8 ± 2° to 115.3 ± 14.8° after sandblasting. The large deviation of this value after sandblasting indicated a significant effect of the sandblasting condition on the surface property of the samples. Therefore, sandblasted samples with larger contact angles were selected for the further treatment. The surface property change after sandblasting is associated with the formation of the microstructures on the paint film. As shown in the SEM image (Fig. 2), rough surface decorated with protuberances at sizes of 5 to 10 μm was created after the paint surface was sandblasted.

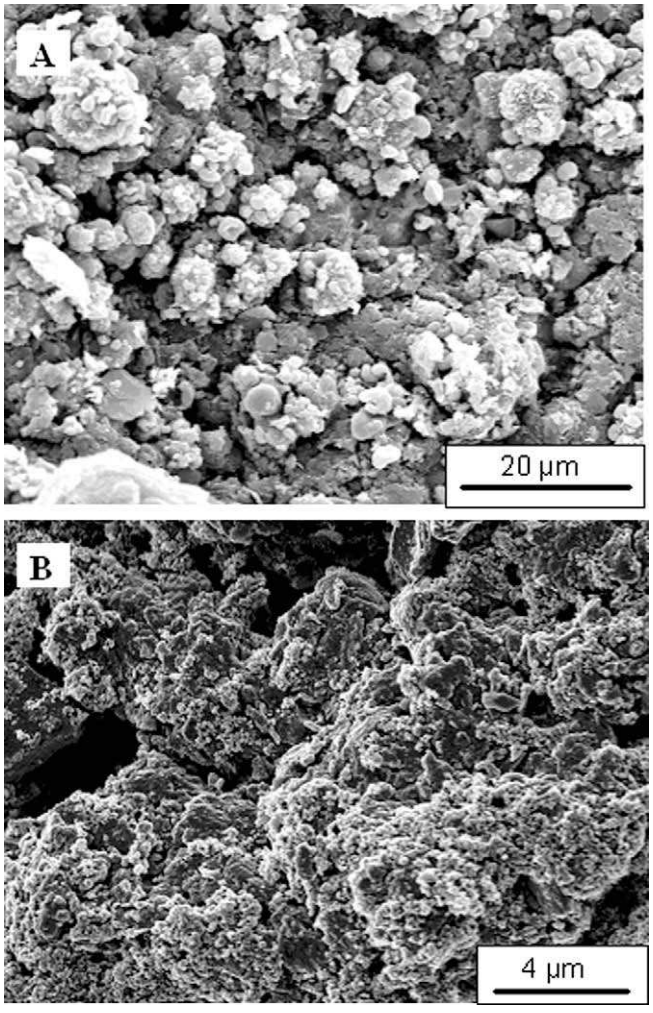

Fig. 2. SEM images of the sandblasted surface of epoxy paint (A) and after it was dip-coated with M1 solution containing 0.5% epoxy adhesive and 0.5% nano-SiO_2 (B).

3.2. The effect of the nano-SiO_2 concentration in M1 on the hydrophobicity

On these sandblasted microstructure surface, nanostructures were then introduced by dip-coating with M1 solution. Fig. 2 demonstrated the change of the surface structure. After this processing, the microstructures surface was anchored with a layer of the SiO_2 nano-particles, while the surface microstructure feature was remained with part of small gaps between the micron size protuberances filled up. M1 solution for dip-coating was a mixture of nano-SiO_2 and epoxy adhesive and was prepared by mixing a nano-SiO_2 solution with an epoxy adhesive solution in 1:1 volume ratio. The epoxy adhesive plays two important roles in this coating process. One is acting as an adhesive to anchor the nano-SiO_2 onto the sandblasted paint surface, and the other is as a coating layer to cover the hydrophilic SiO_2 nano-particle surface to offer a relative hydrophobic surface. It should be noted that about 15 mol% less than stoichiometric amount of the curing agent has been used in the adhesive formulation, so that the resulted adhesive and coating layer were expected to have a low crosslinking density and hence to be more flexible and durable.

On the other hand, the ratio of nano-SiO_2 to epoxy adhesive has to be carefully selected. In M1 solution, at a selected nano-SiO_2 concentration (such as 0.5%), the epoxy concentration should be high enough to efficiently anchor SiO_2 nano-particles onto the microstructures surface and also to sufficiently form a coating layer on the nano-particles. Meanwhile, this concentration should be kept as low as possible to maintain the formed nanostructures. Fig. 3A and B illustrated the influence of the epoxy concentration to the nanostructures. When the sample was prepared from a solution contain 0.5% SiO_2 nano-particles and 0.5% epoxy resin (Fig. 3B), nice nano-particle anchored structures with nano-size grooves formed between the nano-particles were created on the microstructure surface. It should be noted that the sample for Fig. 3B has been further coated with a M2 solution. But the M2 coating did not create any noticeable change in SEM image, which will be further discussed in later section. Therefore, Fig. 3B was used for the discussion on this sample before and after coating with M2. However, when the epoxy resin concentration increased to 5%, Fig. 3 A clearly showed that the nano-grooves between the nano-particles were filled up with the adhesive. The test using a series of solutions with different concentrations revealed that the best structure was obtained when the epoxy concentration is in a range from 0.5% to 2.0%. Therefore, 0.5% of E-44 in M1 solution was used throughout for all the rest experiments.

Then, the influence of the concentration of nano-SiO_2 on the contact angles was studied at the fixed epoxy adhesive concentration (0.5%) in M1 solution. The results were illustrated in Fig. 4. As the nano-SiO_2 concentration increased from 0.0% to 0.1%, the contact angle quickly increased from 115.3° to 151.8°, and then leveled off in the range from 0.1% to 0.75% with the maximum of 154.9° appeared at 0.5%, then it decreases gradually and reaches about 60° at 2.5%. It should be noted that the last value is even much smaller than that on the parent epoxy paint film. This phenomenon is associated with the different states of the anchored nano-SiO_2 layer on the surface formed at different nano-SiO_2 concentrations. The SEM study (not shown) indicated that the surface coated with 0.1% nano-SiO_2 solution only produced a surface partially covered with SiO_2 nano-particles, similar to the result reported in Ref. [38]. As the nano-SiO_2 concentration increased to 0.5%, Fig. 3B showed that the surface was completely covered with

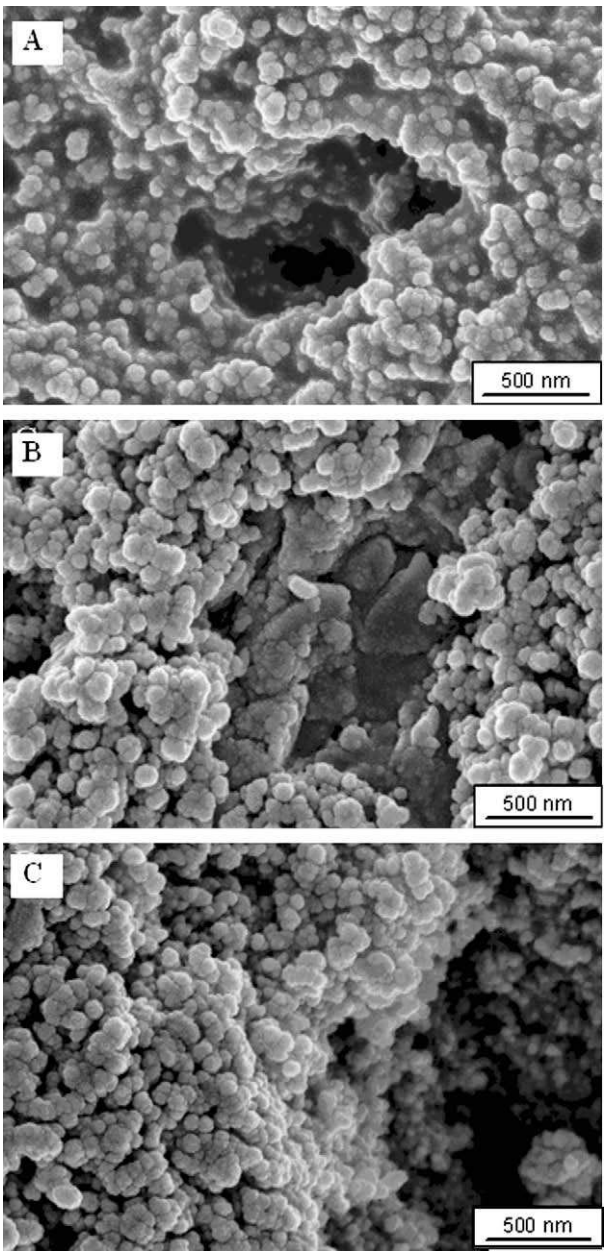

Fig. 3. SEM images of the sandblasted paint surfaces: (A) dip-coated with M1 solution containing 5% epoxy adhesive and 0.5% nano-SiO_2, (B) dip-coated with M1 solution containing 0.5% epoxy adhesive and 0.5% nano-SiO_2 and then with M2 (0.2%) solution, (C) sample B after scouring for 4 h.

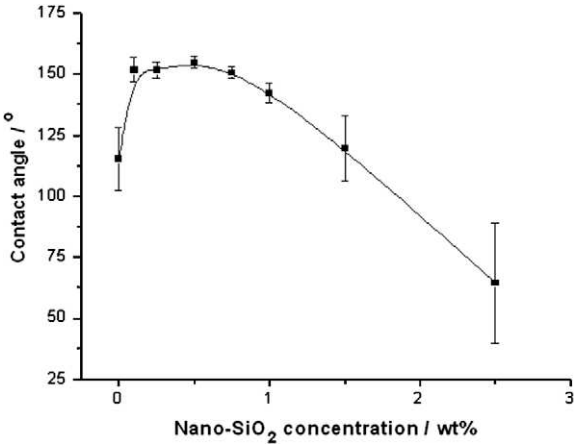

Fig. 4. The relationship between the concentration of nano-SiO_2 and the apparent contact angles.

the nano-particles. In this case, multi-scale nano/microstructures formed on the surface, where the sandblasted paint surface with 5–10 μm microstructures was anchored with a layer of 50–100 nm SiO_2 particles. As the nano-SiO_2 concentration further increased, multilayer nano-particle absorption occurred. It resulted in large part of the micro-cavity filled up with the nano-particles to produce a smoother surface, leading to a decreased contact angle. Furthermore, when the nano-SiO_2 concentration became very high, such as 2.5%, meaning a very low polymer/nano-SiO_2 ratio, the SiO_2 nano-particle surface would not be sufficiently covered with the polymer. It should be noted that SiO_2 is a hydrophilic material with a very low contact angle. The coating of bare SiO_2 nano-particles on the paint surface will create a hydrophilic surface with a low contact angle [38]. The E-44 concentration in the solution is only 0.5%. When the nano-SiO_2 concentration in the solution is low, such as 0.5%, the ratio of polymer to nano-SiO_2 is about 1:1. With the particle size of the nano-SiO_2 being ~15 nm, a complete and uniform coating of the polymer on the nano-particles only produces a ~2 nm thick layer. Apparently this value is too low for forming a sufficient coating layer to screen off the hydrophilic property of SiO_2. Fortunately, Fig. 3 indicates that the anchored SiO_2 nano-particles on the surface have a size of 50–100 nm, meaning they are not in the form of single particles, but in the form of agglomerated particles containing about 30–300 primary nano-particles of ~15 nm size. Actually the SiO_2 nano-particles in the dry state are agglomerated to form larger sizes due to their huge surface energy. Ultrasonicating the nano-SiO_2 in a solution re-dispersed the agglomerates to smaller size of 50–100 nm. In this case, under the given concentration, the coating layer on the particle surface could be 7–13 nm thick, which is sufficient to form a complete coating layer. Further increasing the concentration of nano-SiO_2 means reducing the ratio of polymer to nano-particles, and causes a fraction of the hydrophilic surface of the nano-SiO_2 without a coating layer, resulting in a low contact angle as for the sample prepared from 2.5% nano-SiO_2 solution. Therefore, the decrease of the contact angle is a result of the following two effects caused by the increase of the nano-SiO_2 concentration: One is the lower micro-size roughness of the surface due to the multilayer absorption of nano-particles, which will fill up the micro-cavities on the surface. The other is the less perfect polymer coating layer on the nano-particles.

3.3. The effect of the concentration of M2 solution on the superhydrophobicity

The highest contact angle observed on M1 coated surfaces is about 154°, which is not as high as many reported superhydrophobic surface. The main reason for this low value is the low hydrophobicity of the coating material, the epoxy adhesive used in M1, which contains high content of polar groups and has a high surface energy with a contact angle of 78°. An improvement of the superhydrophobicity can be expected when the epoxy coating layer was replaced by a low surface energy material. Therefore, the obtained M1 coated surface was further coated with M2, an ATPS modified epoxy adhesive solution, containing 30 wt.% of polydimethylsiloxane (PDMS) chains in the polymer. PDMS has a very low surface energy with a water contact angle of 109° [39]. Its segments in the coating layer have high tendency to enrich on the surface to promote the hydrophobicity because of its incompatibility with the epoxy matrix [40,41].

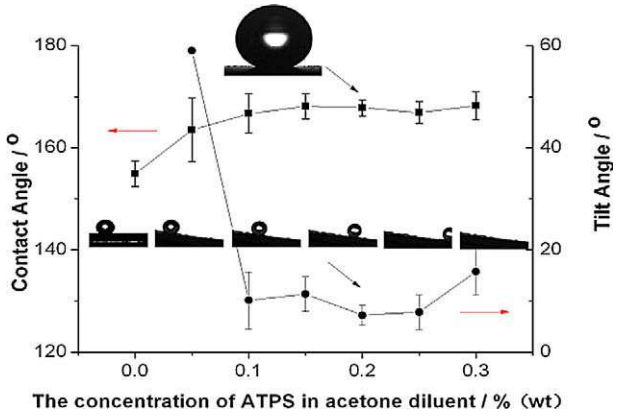

Fig. 5. The relationship of the superhydrophobicity with the ATPS concentration (The sample without M2 coating was marked as 0% sample, its sliding angle is larger than 90°).

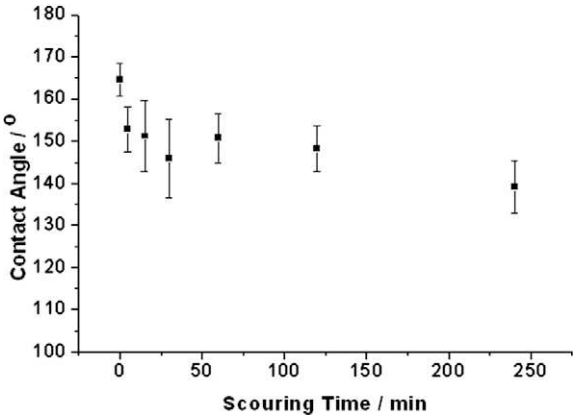

Fig. 6. The variation of the apparent contact angle versus the scouring time.

The influence of the M2 coating on both of the apparent contact angle and the sliding angle has been studied, and the results were illustrated in Fig. 5 in terms of apparent contact angle and sliding angle varied with the ATPS concentration in the solution. It can be seen that coating with M2 solutions efficiently increases the apparent contact angle from 154° to above 160° in the whole tested concentration range from 0.05% to 0.3%. When the ATPS concentration becomes larger than 0.1%, the value of the contact angle reach almost constant, indicating a complete coverage of the M2 layer on the surface at this concentration. This observation can be further confirmed by the sliding angle test. Although the untreated M1 surface displays a high contact angle (154°), the sliding angle as high as 90° is found on this surface. This phenomenon implies water has a very strong interaction with the surface, and hence it is more close to "Wenzel" regime [31], attributing to the relative hydrophilic property of the epoxy resin. After dip-coating with M2 solution, the surface showed a dramatically reduced sliding angle of ~60° at 0.05% of ATPS concentration, and then it further jumped to 10° at 0.1%. After then, the concentration increase only slightly reduce this value to 7° at 0.2%, but this value was inversely increased to 16° at 0.3%, This phenomenon is believed to be related to partially lost of the nano-size surface roughness due to over coating of the polymer [42]. Though this change was not clearly verified by SEM study for the sample dip-coating with

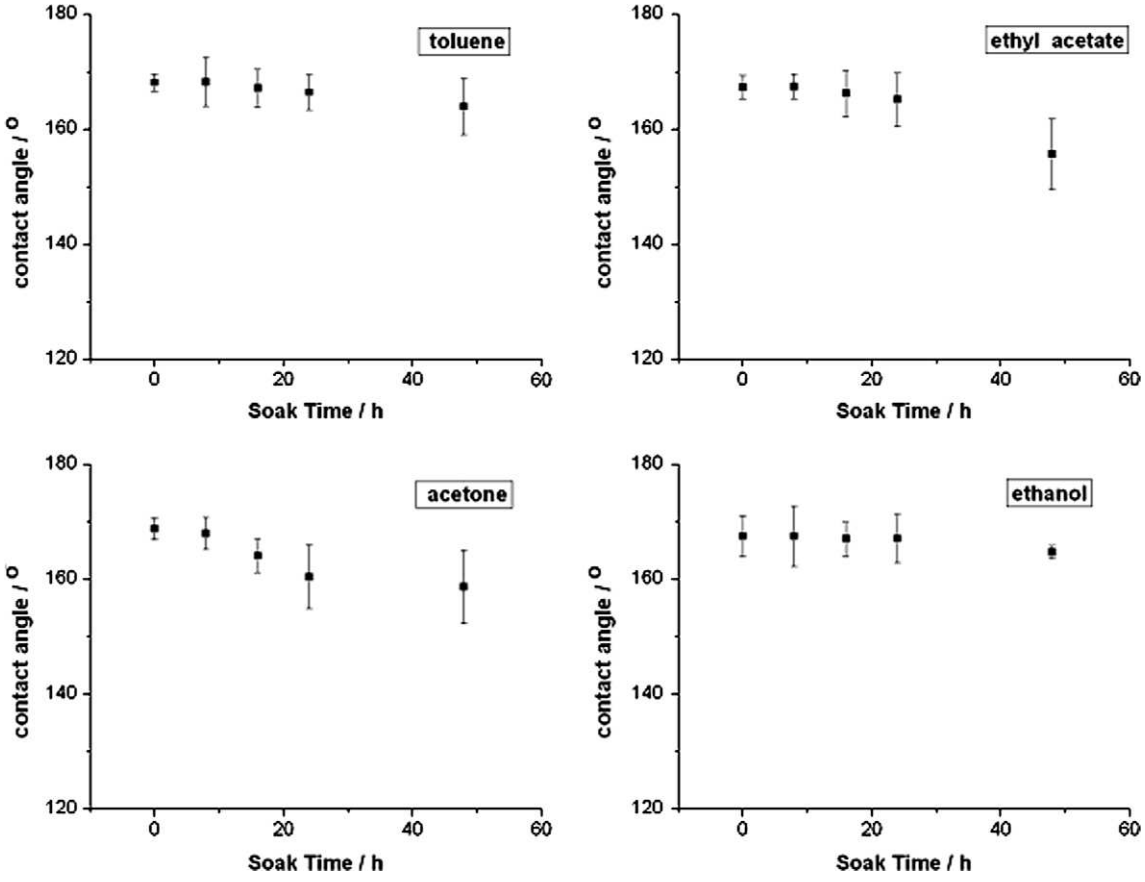

Fig. 7. The variation of the apparent contact angle of the as-prepared superhydrophobic surface with soaking time.

0.05–0.3% M2 solution. This result confirms that 0.1% of ATPS concentration of M2 solution is sufficient to modify the surface property and 0.2% of the concentration gives the optimized result in producing surface with the smallest sliding angle. This result also confirms that the material on the surface with a low surface energy is very importance to convert the surface from Wenzel to Cassie regime.

3.4. The resistance against water scouring

The durability of the produced superhydrophobic surface has been tested by a water scouring test, where the M2 coated samples were scoured by water current at a speed of 10 m/s, which is an extremely harsh condition to mimic a torpedo in water. Fig. 6 showed the changes of the contact angles of the surface versus the scouring time. During the first 5 min of the test, the contact angle had an obvious decrease, reduced about 12°. It might be resulted from the loose particles being washed off the surface by the current, which generated a slightly reduced roughness of the surface [19]. Then the contact angle only showed a very little decrease as the scouring time increased, with the value remained at about 140° at last, indicating a good durability of the superhydrophobic property against the water scouring. The SEM study of the sample before and after scouring as shown Fig. 3B and C confirmed this result. It did not show apparent changes of the structure after the scouring test. This excellent stability is attributed to the excellent mechanical strength of epoxy adhesive associated with the crosslinked structure as well as the strong interaction between epoxy adhesive and SiO_2. However, the sliding angle of the surface increased significantly with the scouring time. The sliding angle increased to 20° in 5 min. After 4 h scouring, 10 μL water droplets can stick on the most of the area of the surface, indicating a sliding angle larger than 90°. Base on Furmidge's equation (Eq. (3)), this phenomenon indicates water has very strong interaction with the surface, implying thin coating layer on the nano-particle surface was washed off during the long time scouring test, and the surface was converted from Cassie regime to Wenzel regime. Therefore, we can conclude: though the epoxy adhesive is strong enough to maintain the SiO_2 nano-particles on the surface after 4 h high speed water scouring, the epoxy coating layer on the nano-particles surface can only be remained for a short time, such as 5 min. It can be removed in a longer scouring time. This must be associated with the high polarity of both SiO_2 surface and epoxy coating. In addition with the very thin coating layer in thickness, water molecules can penetrate through the coating layer to accumulate on the SiO_2 surface to make the coating layer easily peeled off by high speed water current. However, this change was not clearly seen in SEM (Fig. 3). It might due to the coating layer being not thick enough to be detected by the SEM.

3.5. Chemical resistance of the superhydrophobic surface

The solvent resistance of the M2 modified superhydrophobic surface was tested by immersing the samples in four common organic solvents (toluene, ethyl acetate, acetone, ethanol) for two days. The result is displayed in Fig. 7. The water contact angles of the samples in toluene and ethanol only displayed a very small change in two days, while those of the samples soaked in acetone and ethyl acetate were decreasing apparently along with the soaking time. This phenomenon might be attributed to the stronger solvating property of acetone and ethyl acetate to the epoxy coating layer, the higher swollen of the polymer in these two solvents will damage the very thin coating layer on the SiO_2 nano-particles.

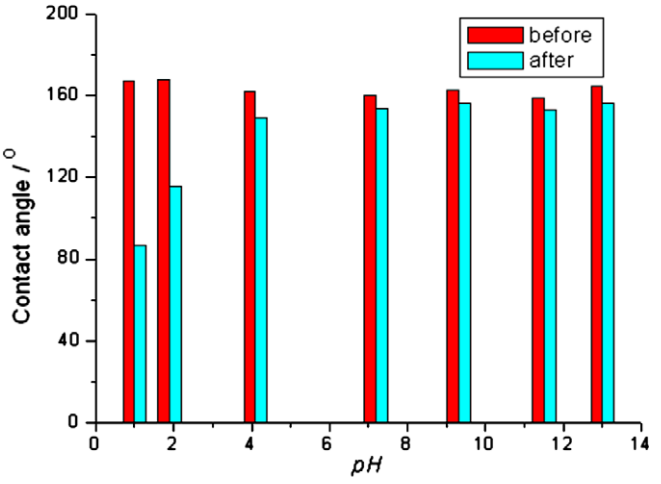

Fig. 8. The apparent contact angle of the surface before and after soaked in acidic and basic aqueous solutions for 1 day.

Fig. 8 shows the apparent contact angle of the prepared surfaces before and after soaked in aqueous solutions with different pH values for 1 day. The samples are sensitive to the acidity of the solution with the pH value lower than 4.0. There is a rapid decrease in the contact angles for the soaked samples. A stronger acidic solution resulted in a greater decrease of the contact angles. After soaked in the solution at pH = 1, the contact angle sharply decreases from nearly 170° to about 87°. The hydrolytic cleavage of the Si–O–C bonds on the polymer/SiO_2 interface by acid should be responsible for this phenomenon. After hydrolysis, hydrophilic hydroxyl group will occupy the SiO_2/polymer interface, leading to the removal of the M1 and M2 coating layer and then decrease in the hydrophobicity of the surface. Meanwhile, the contact angle did not show a dramatic change in the solutions with a pH value larger than four, indicating a high resistance of this system towards water and moisture.

3.6. The uniformity of the as-prepared superhydrophobic surface

The uniformity of a large scale sample was evaluated by a multi-spot contact angle measurement. A sample in a size of $120 \times 40\ mm^2$ (which is the largest sample suitable for the test with the contact angle meter) was prepared. Ninety six testing points have been selected on the sample, which are uniformly

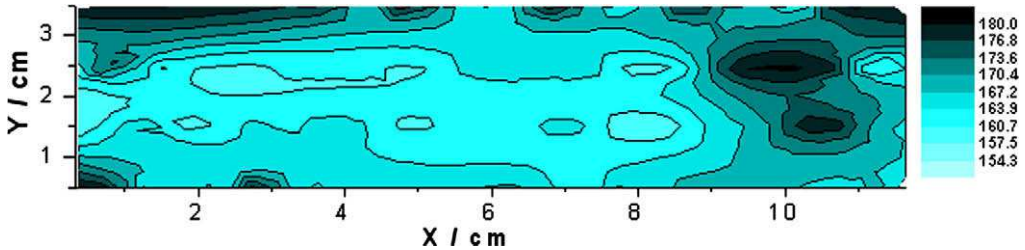

Fig. 9. The uniformity of superhydrophobicity on the as-prepared surface.

dispersed on the surface with two spots per square centimeter. The statistical average contact angle is 166.7° ± 6.7°and the dispersion rate of the data on the whole surface is within 5% (Fig. 9). Thus, the as-prepared samples possess uniform enough superhydrophobcity for large scale sample preparation.

4. Conclusions

A series of superhydrophobic surfaces on epoxy paints have been successfully constructed by a three-step procedure through sandblasting to construct microstructure, anchoring nano-SiO_2 to construct nano-structure, and dip-coating with ATPS modified epoxy adhesive for reducing the surface energy. The apparent contact angles on the prepared surfaces can reach as high as 167.8 ± 1.6. And the sliding angles can reach as low as 7.2 ± 1.9. The results demonstrate that low surface energy materials and multi-scale micro- and nanostructures are two essential factors in the preparation of superhydrophobic surfaces with low sliding angles. This process has been used to prepare larger scale samples to produce surface with highly repeatable contact angle values in the whole area. The superhydrophobic surface also shows an excellent stability against high speed scouring tests, soaking in neutral and basic aqueous solutions, and common organic solvents such as toluene and ethanol.

References

[1] A.B.D. Cassie, Discuss. Faraday Soc. 3 (1948) 11.
[2] R.N. Wenzel, Ind. Eng. Chem. 28 (1936) 988.
[3] C.G.L. Furmidge, J. Colloid Sci. 17 (1962) 309.
[4] T.L. Sun, L. Feng, X.F. Gao, L. Jiang, Acc. Chem. Res. 38 (2005) 644.
[5] Z.G. Guo, W.M. Liu, Plant Sci. 172 (2007) 1103.
[6] C. Neinhuis, W. Barthlott, Ann. Bot. 79 (1997) 667.
[7] X.F. Gao, L. Jiang, Nature 432 (2004) 36.
[8] A. Scardino, R. De Nys, O. Ison, W. O'Connor, P. Steinberg, Biofouling 19 (2003) 221.
[9] T. Kako, A. Nakajima, H. Irie, Z. Kato, K. Uematsu, T. Watanabe, K.J. Hashimoto, Mater. Sci. 39 (2004) 547.
[10] M. Zielecka, E. Bujnowska, Prog. Org. Coat. 55 (2006) 160.
[11] X.J. Feng, L. Feng, M.H. Jin, J. Zhai, L. Jiang, D.B. Zhu, J. Am. Chem. Soc. 126 (2004) 62.
[12] N.J. Shirtcliffe, G. McHale, M.I. Newton, G. Chabrol, C.C. Perry, Adv. Mater. 16 (2004) 1929.
[13] F. Xia, L. Jiang, Adv. Mater. 20 (2008) 2842.
[14] C. Badre, P. Dubot, D. Lincot, T. Pauporte, M. Turmine, J. Colloid Interface Sci. 316 (2007) 233.
[15] H.M. Bok, S. Kim, S.H. Yoo, S.K. Kim, S. Park, Langmuir 24 (2008) 4168.
[16] Y.K. Lai, C.J. Lin, J.Y. Huang, H.F. Zhuang, L. Sun, T. Nguyen, Langmuir 24 (2008) 3867.
[17] Q.J. Wang, Z. Cui, Y. Xiao, Q.M. Chen, Appl. Surf. Sci. 253 (2007) 9054.
[18] L.L. Cao, T.P. Price, M. Weiss, D. Gao, Langmuir 24 (2008) 1640.
[19] Z. Cui, Q.J. Wang, Y. Xiao, C.H. Su, Q.M. Chen, Appl. Surf. Sci. 254 (2008) 2911.
[20] Q. Wang, B.W. Zhang, M.N. Qu, J.Y. Zhang, D.Y. He, Appl. Surf. Sci. 254 (2008) 2009.
[21] O.U. Nimittrakoolchai, S. Supothina, J. Eur. Ceram. Soc. 28 (2008) 947.
[22] D.K. Sarkar, M. Farzaneh, R.W. Paynter, Mater. Lett. 62 (2008) 1226.
[23] A. Ruiz, A. Valsesia, G. Ceccone, D. Gilliland, P. Colpo, F. Rossi, Langmuir 23 (2007) 12984.
[24] T.N. Krupenkin, J.A. Taylor, E.N. Wang, P. Kolodner, M. Hodes, T.R. Salamon, Langmuir 23 (2007) 9128.
[25] R.D. Mundo, F. Palumbo, R. d'Agostino, Langmuir 24 (2008) 5044.
[26] R. Menini, M. Farzaneh, Polym. Int. 57 (2008) 77.
[27] L. Feng, Y.L. Song, J. Zhai, B.Q. Liu, J. Xu, L. Jiang, D.B. Zhu, Angew. Chem. Int. Ed. 42 (2003) 800.
[28] Y.I. Yoon, H.S. Moon, W.S. Lyoo, T.S. Lee, W.H. Park, J. Colloid Interface Sci. 320 (2008) 91.
[29] Z.Q. Yuan, H. Chen, J.D. Zhang, Appl. Surf. Sci. 254 (2008) 1593.
[30] A.D. Sommers, A.M. Jacobi, J. Micromech. Microeng. 16 (2006) 1571.
[31] P. Roach, N.J. Shirtcliffe, M.I. Newton, Soft Matter 4 (2008) 224.
[32] S. Wang, L. Feng, L. Jiang, Adv. Mater. 18 (2006) 767.
[33] C.F. Wang, Y.T. Wang, P.H. Tung, S.W. Kuo, C.H. Lin, Y.C. Sheen, F.C. Chang, Langmuir 22 (2006) 8289.
[34] Z. Guo, F. Zhou, J. Hao, W.J. Liu, J. Am. Chem. Soc. 127 (2005) 15670.
[35] Y.Y. Wu, M. Bekke, Y. Inoue, H. Sugimura, H. Kitaguchi, C.S. Liu, O. Takai, Thin Solid Films 457 (2004) 122.
[36] B.S. Hong, J.H. Han, S.T. Kim, Thin Solid Films 351 (1999) 274.
[37] X.M. Li, D. Reinhoudt, M. Crego-Calama, Chem. Soc. Rev. 36 (2007) 1350.
[38] W.X. Hou, Q.H. Wang, J. Colloid Interface Sci. 316 (2007) 206.
[39] H.L. Cong, T.R. Pan, Adv. Funct. Mater. 18 (2008) 1912.
[40] R.S. Chen, C.J. Chang, Y.H. Chang, J. Polym. Sci. Part A Polym. Chem. 43 (2005) 3482.
[41] M. Horgnies, E. Darque-Ceretti, Prog. Org. Coat. 55 (2006) 27.
[42] C.F. Wang, Y.T. Wang, P.H. Tung, S.W. Kuo, C.H. Lin, Y.C. Sheen, F.C. Chang, Langmuir 22 (2006) 8289.